

Performance-based probabilistic framework for seismic risk, resilience, and sustainability assessment of non-ductile RC structures

Ghazanfar Ali Anwar¹, You Dong^{2, *}, and Changhai Zhai³

Abstract:

Recent earthquakes have highlighted additional losses due to the lack of resilience of damaged structures. Environmental impact, as performance indicator, has also received increased attention within performance-based earthquake engineering. In this paper, a combined probabilistic framework is proposed to assess seismic risk, sustainability and resilience of a non-ductile reinforced concrete frame structure. The framework utilizes three-dimensional inelastic fiber-based numerical modeling approach to develop limit states associated with performance levels. The decision variables (i.e. repair cost, downtime and equivalent carbon emissions) are quantified at both component- and system-level, and are compared considering seismic risk, sustainability, and resilience. Additionally, the proposed approach considers uncertainties in the building performance and consequence functions of structural and non-structural components. Fast-track and slow-track schemes are utilized as a repair strategy and probabilistic resilience is quantified given the investigated time period. The proposed approach can aid the development of next generation of performance-based engineering incorporating both resilience and sustainability.

Keywords: Resilience; Sustainability; RC buildings; Equivalent carbon emissions; Performance-based engineering; Loss estimation

¹ Research Assistant and Ph.D. student, The Hong Kong Polytechnic University, Department of Civil and Environmental Engineering, Hung Hom, Kowloon, Hong Kong, ghazanfar-ali.anwar@connect.polyu.hk

² Assistant Professor of Structural Engineering, The Hong Kong Polytechnic University, Department of Civil and Environmental Engineering, Hung Hom, Kowloon, Hong Kong, you.dong@polyu.edu.hk.

³ Key Lab of Structures Dynamic Behavior and Control of the Ministry of Education, Harbin Institute of Technology, Harbin, China; Key Lab of Smart Prevention and Mitigation of Civil Engineering Disaster of the Ministry of Industry and Information Technology, Harbin Institute of Technology, Harbin, China, zch-hit@hit.edu.cn

*Corresponding Author.

1. Introduction

Conventional strength design methods provides the intended life safety function but can result in extensive structural and non-structural damage causing economic losses due to downtime and repair (Ellingwood, 2006; Zhai et al., 2015; Frangopol et al., 2017; Padgett and Li, 2014; Padgett and Tapia, 2013), as was observed during 1994 Northridge and 1995 Kobe earthquakes (duPont IV and Noy, 2015). Pacific Earthquake Engineering Research (PEER) methodology can be used to determine cost of repair (FEMA, 2012). The additional losses of an earthquake due to downtime have not yet been fully explored. Hence, new measures need to be defined and quantified. The 1994 Northridge, California, and 1995 Kobe, Japan earthquakes concluded, that life safety limit state can be achieved using conventional design methods, but can have huge economic consequence, not only limited to the immediate aftermath of an earthquake but also to the recovery phase of a building (Miles and Chang, 2006). Performance based earthquake engineering (PBEE) methodology provides cost of repair in an earthquake event, which can be used to assess and reduce the immediate economic losses, but the indirect economic losses needs further investigation (Bocchini et al., 2013; Dong et al., 2013; Zheng and Dong, 2018). In this paper, both the direct (i.e. losses due to the repair activities) and indirect losses (i.e. additional losses due to inability of infrastructure to be functional), associated with structural damage and its repair are considered within the PBEE.

Resilience is used to account for robustness and efficient recovery of a building. In the context of built environment, Bruneau et al. (2003) provided a definition focusing on the social systems to adapt and recover hazard events. While most of the research focus is on lifeline infrastructures, e.g., water networks (Herrera et al., 2016), gas networks (Carvalho et al., 2014), electricity and transportation networks (Alipour and Shafei, 2016; Sun et al., 2018; Dong and Frangopol, 2017; Qeshta et al., 2019), fewer studies have been devoted for the disaster recovery of building infrastructure. The first step towards a resilient community is to understand individual infrastructure components and its relation to a whole community. Broccardo et al. (2015) presented probabilistic resilience assessment methodology of civil systems, and Burton et al. (2015) proposed a PBEE methodology for the recovery process associated with a building community. Lin and Wang (2017a; 2017b) developed a methodology for recovery modeling by aggregating building-level restoration using probabilistic damage assessment. Similar approach is generally utilized for the resilience evaluation (Koliou et al., 2017; Masoomi and van de Lindt, 2018) and few studies utilizes detailed component-based damage and consequence assessment approach to quantify resilience (Dong and Frangopol, 2016; Hashemi et al., 2019). In this paper, nonlinear time-history analysis is conducted to assess the performance at both component and system levels utilizing next-generation PBEE. Then, given damaged functionality and recovery scheme, the resilience is quantified.

Sustainability addresses social, economic and environmental issues and its impact on the future generations (Sabatino et al., 2015; Zhao et al., 2014). Structures constructed in hazard prone regions needs to be resilient to fulfil sustainability objectives (Zheng et al., 2018; Wen et al., 2019). Resilience and sustainability have vast similarities and should be used in an integrated perspective (Bocchini et al., 2013; Rodriguez-Nikl, 2015). Frameworks for the resilience and sustainability have been developed (Marchese et al., 2018) and studies are available incorporating sustainability in hazard prone regions (Gencturk et al., 2016; Asprone and Manfredi, 2015). However, a computational platform incorporating seismic sustainability and resilience using detailed component-level damage assessment model is limited. Moreover,

there is an increasing trend to incorporate uncertainties in the seismic sustainability and resilience assessment procedures. The uncertainties in hazard model arise because of inability to accurately predict hazard, structural models and damage assessment are also associated with uncertainties. Additionally, there are uncertainties associated with consequences resulting from repair actions, downtime, and carbon emissions, among others. The cumulative result of these inherent uncertainties makes precise evaluation difficult and uncertainties should be accounted. To the best knowledge of authors, there have been very limited studies investigating seismic sustainability and resilience of non-ductile residential building utilizing physics-based building fragilities and component-level damage assessment, except for few. For instance, Hashemi et al. (2019) investigated seismic sustainability and resilience of limited-ductile RC building. A multi-axis hybrid simulation was performed and CFRP retrofit was investigated in detail. Structural damage states were defined experimentally, and performance-based methodology was used to incorporate resilience into life-cycle sustainability approach. There is a further need to incorporate comprehensive structural and non-structural components in the component-based performance assessment methodology. Additionally, there exist uncertainties in seismic sustainability and resilience and a probabilistic platform is required to present results. In comparison, the current study evaluates seismic sustainability and resilience probabilistically considering the uncertainties in the framework by using lognormal or normal distributions of repair cost, repair times, and equivalent CO₂ emissions.

In this paper, a probabilistic seismic sustainability- and resilience-informed assessment methodology is developed and applied to a non-ductile RC frame structure utilizing next-generation performance-based assessment procedures. Non-ductile building refers to a structure with inadequate detailing and reinforcing steel and is not designed considering the seismic provisions. This paper focuses on PEER methodology accompanied with detailed non-linear fiber-based models for accurate prediction of spread of nonlinearity utilizing incremental dynamic analysis (IDA) to account for numerical instabilities under suits of earthquake records. Nonlinear time history analyses are performed, and seismic risk and sustainability are quantified in terms of repair cost, carbon emissions, and downtime using damage fragility and consequence functions of structural and non-structural components. The uncertainties associated with consequence functions are incorporated, and probabilistic resilience is quantified. The proposed approach is illustrated by dividing the paper into five sections. Section 2 introduces seismic sustainability and resilience. Section 3 presents performance-based seismic assessment methodology used for the component-level damage assessment and recovery. In Section 4, the proposed approach is illustrated on a multi-unit residential eight story RC frame non-ductile building. The last section presents conclusions of the paper.

2. Seismic sustainability and resilience

2.1. Seismic sustainability

Sustainability, as defined in the report of Brundtland, (1987) is “meeting the needs of present generation without compromising the ability of future generations to meet their own needs”. Sustainability assessment include social, economic and environmental impacts distributed over life-cycle of a building (e.g., construction, maintenance, demolition, ageing). In this study, the seismic sustainability is emphasized by considering the socio-economic and environmental impacts resulting from earthquake hazard. Environmental indicator (e.g., equivalent carbon emissions) is used to evaluate environmental impacts. Social impact of seismic sustainability

is determined by calculating total repair time of a building under seismic hazard. Mathematically, the sustainability impact of earthquake hazard can be computed as:

$$SI = C_{SM|C} \cdot p_{C|IM} + C_{SM|NC} \cdot (1 - p_{C|IM}) \quad (1)$$

$$C_{SM|NC} = \sum_{Comp} \sum_{DS} C_{SM,Comp|DS} \cdot p_{DS,Comp|IM} \quad (2)$$

where $C_{SM|C}$ and $C_{SM|NC}$ is the consequence (e.g., economic loss, equivalent CO₂ emissions, repair time) given collapse and non-collapse of a building; IM is the intensity measure; $p_{C|IM}$ is the probability of collapse under IM ; $C_{SM,Comp|DS}$ is the sustainability metric given a damage state of a given component with the building; and $p_{DS,Comp|IM}$ is the probability of a damage state associated with component under given IM .

The carbon emissions due to repair (i.e. non-collapse condition) are accounted for, by calculating probability of damage states (i.e. $p_{DS,Comp|IM}$) utilizing fragility functions of considered structural and non-structural components. The consequences associated with different repair actions are weighted with relevant probability of being in damage states to determine desirable sustainability impact of a particular component (i.e. $\sum_{DS} C_{SM,Comp|DS} \cdot p_{DS,Comp|IM}$). Similar procedure is carried out for all the components and the desirable consequences given non-collapse of a building are evaluated (i.e. $C_{SM|NC}$). The consequence given collapse of a building is determined considering construction materials (e.g. concrete, reinforcing steel, bricks) used during the construction phase and the relevant sustainability impact of construction materials can be determined. The total sustainability impact (e.g. equivalent carbon emissions) is evaluated by adding consequences for collapse and non-collapse of a building weighted as represented in Eq. (1).

2.2. Resilience

Resilience is represented by its functionality and can be associated with four attributes: *robustness*: the ability to withstand an extreme event without complete failure; *rapidity*: the ability to recover from an extreme event efficiently and effectively; *redundancy*: reserve or substitutive structural components or systems; and *resourcefulness*: efficiency in identifying problems, prioritizing solutions, and mobilizing (Bruneau et al., 2003). Mathematically, resilience can be evaluated by integrating the functionality curve over time as indicated in Figure 1.

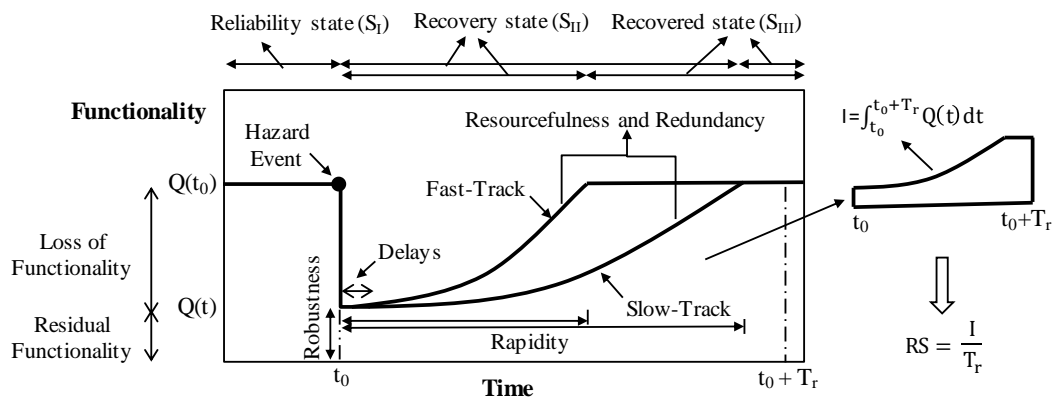


Figure 1. Resilience assessment under hazards

$$RS = \frac{1}{T_r} \int_{t_0}^{t_0+T_r} Q(t)dt \quad (3)$$

where $Q(t)$ is the functionality; t_0 is the time of occurrence of the extreme event and T_r is the time of investigation of functionality. As shown in Figure 1, the three functionality states associated with the functionality are proposed defined as follows:

- (1) Reliability state (S_I): Pre-event functionality state where building is considered to have baseline functionality (i.e., the building is functional or in an original state before the occurrence of a hazard event);
- (2) Recovery state (S_{II}): Post-event functionality state where the building is considered to have loss of functionality depending upon the robustness of the building, and time variant functionality regain as a result of repair efforts. Two types of repair schemes are defined for functionality recovery (i.e., series repair scheme where building is repaired one story at a time termed as slow-track and parallel repair scheme where all the stories are repaired simultaneously termed as fast-track). The repair efforts are an attribute of resourcefulness and redundancy of the system; and
- (3) Recovered state (S_{III}): building functionality after the recovery efforts (i.e., building regains loss of functionality)

In the reliability state, the building has baseline functionality and at t_0 the building changes from baseline functionality to residual functionality as a result of physical damage and loss of services of a building. After a hazard event, state changes from reliability state to recovery state, which includes the delay time (i.e., time required for inspection, engineering mobilization, review and/or redesign, financing, contractor mobilization and permitting etc.) and the time-variant functionality improvement. Subsequently, repair actions are performed, and the building regains its functionality to reach recovered state. The resilience can be calculated by taking integral from a hazard event to the investigated time period.

3. Integrated performance-based engineering incorporating sustainability and resilience

The PBEE methodology is carried out in four stages (i.e., hazard, structural, damage, and loss analysis), providing Decision Variables (DVs) meaningful to the stakeholders. Figure 2 explains the integrated methodology from hazard identification to seismic risk, sustainability, and resilience quantification. The methodology focuses on the probabilistic procedures to incorporate uncertainties in all phases of the process.

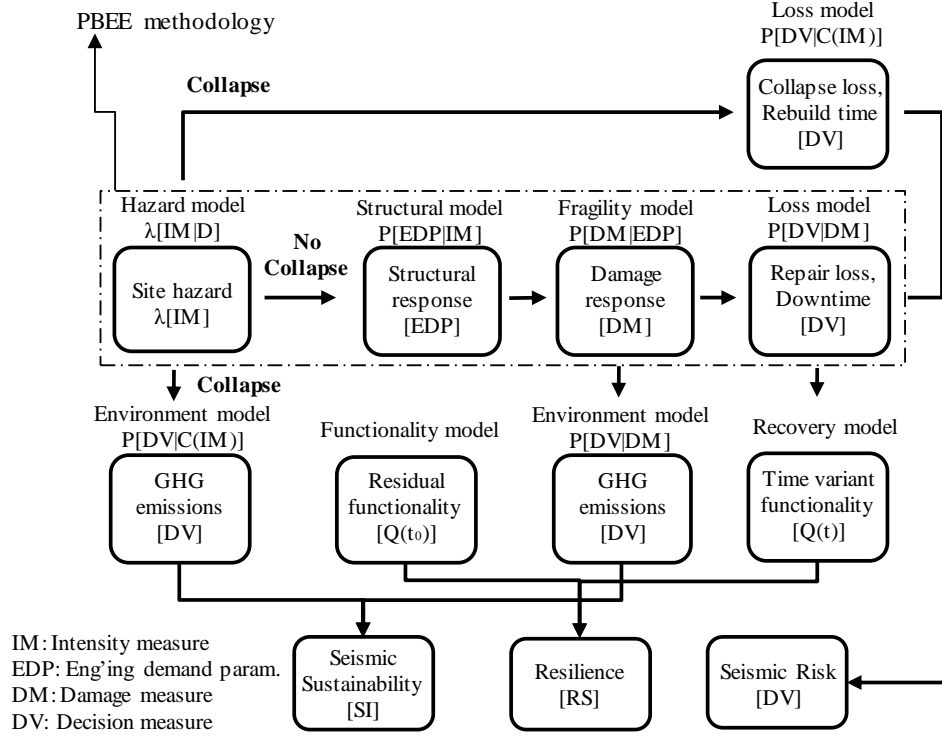


Figure 2. PEER PBEE methodology incorporating sustainability and resilience

Each stage of PBEE methodology is carried out individually to arrive at DVs. For a given earthquake scenario, eqs. (4-6) are used to calculate expected total loss, total repair time and total sustainability impact (e.g. environmental indicator in terms of equivalent carbon emissions).

$$L_{T|IM} = L_{C|IM} + L_{NC|IM} \quad (4)$$

$$RT_{T|IM} = RT_{C|IM} + RT_{NC|IM} \quad (5)$$

$$SI_{T|IM} = SI_{C|IM} + SI_{NC|IM} \quad (6)$$

where $L_{T|IM}$ is a total monetary loss DV; $L_{C|IM}$ and $L_{NC|IM}$ are losses for collapse and non-collapse; $RT_{T|IM}$ is a total building repair time DV; $RT_{C|IM}$ and $RT_{NC|IM}$ are repair times for collapse and non-collapse; $SI_{T|IM}$ is the total seismic sustainability impact (e.g., equivalent carbon emissions); and $SI_{C|IM}$ and $SI_{NC|IM}$ are seismic sustainability impact for collapse and non-collapse cases. The detailed process of PBEE incorporating resilience and sustainability is introduced in the following section.

3.1. Hazard analysis

PBEE methodology requires selection of suits of earthquake records representative of the potential scenarios, a structural system may experience. The representative earthquake records for dynamical analysis are selected based on the criteria, such as magnitude, source mechanism, source to site distance, rupture directivity, and local site conditions, among others (Katsanos et al., 2010). Several ground motion databases are available for ground motion selection, such as PEER ground motion database (Kishida et al., 2018), European strong-motion database (Ambraseys et al., 2004).

3.2. Structural analysis

Structural analysis is performed to evaluate the response of structure under seismic hazard. Nonlinear time history analysis is performed to determine engineering demand parameters (EDP) (such as element forces, deformations, floor accelerations, drifts etc.). Element forces and drifts are considered more suitable for structural components, while peak floor accelerations and peak floor velocities are usually considered for non-structural components. The variation in hazard is incorporated by considering number of analyses with given intensity measures to get mean and variance of EDPs. The probability of collapse $p_{C|IM}$ can be determined using collapsed data from Incremental Dynamic analysis (IDA) (Vamvatsikos and Cornell, 2002) and probability of having no global collapse can be determined using total probability theorem as represented in Eq. (7).

$$p_{NC|IM} = 1 - p_{C|IM} \quad (7)$$

A lognormal cumulative distribution function is used to fit the probability of collapse under a given EDP (Sfahani et al., 2015). Fragility curves for IO, LS, and CP can also be generated in a similar fashion as follows

$$p_{C|IM} = \Phi\left(\frac{\ln(x/\theta)}{\beta}\right) \quad (8)$$

where Φ is the standard normal cumulative distribution function (CDF); θ is the median of the collapse fragility function (i.e., Intensity measure (IM) with 50% probability of collapse); and β is the dispersion or standard deviation of $\ln IM$.

3.3. Damage analysis

Damage analysis is performed to determine physical damage at the component-level using structural responses in terms of EDPs. The probabilistic EDPs are incorporated with the damage fragility curves to calculate Probability of Exceedance (PoE) of damage states. Damage measures (DM) in terms of different damage levels or damage states are typically defined as fragility functions to quantify damage. The damage fragility functions for structural and non-structural components can be developed using experimental testing, analytical modeling and/or expert opinion. Component fragility functions are usually divided into fragility groups and performance groups depending upon the EDPs effect on component damage.

3.4. Seismic risk assessment

Loss analysis is performed to determine direct economic losses and downtime. The PoEs obtained from damage analysis are used to determine losses using consequence functions, which are likely values of repair to replacement cost ratio, repair time, etc. Limit state fragilities are utilized along with the hazard model to determine probability of collapse of a building and related consequences are evaluated. Fragility functions utilized in the fragility model are used along with the repair actions to evaluate related consequences for non-collapse of a building. The uncertainties of the consequence functions are included depending upon the variability in each of the DV. Monte Carlo process is used to generate large number of EDPs for the statistically consistent demand sets given a limited set of input EDPs. These demand sets generated using Monte Carlo simulations are used with fragility and consequence functions to

calculate statically distributed DVs. Losses due to collapse and non-collapse of a building are added to determine seismic risk due to earthquake scenario.

3.5. Seismic sustainability and resilience assessment

The seismic sustainability and resilience assessment incorporated in the proposed framework is outlined in Figure 3. Step 1 starts with building a detailed finite element model. A suit of earthquake ground motions is selected, and IDA is performed to develop fragilities at immediate occupancy (IO), life safety (LS), collapse prevention (CP), and collapse (C) limit states. In Step 2, three hazard scenarios are considered with 50%, 10%, and 2% probability of exceedance in 50 years of a structure. Non-linear time history analyses are performed to evaluate structural responses (e.g., story drifts, floor accelerations, and velocities). Drift sensitive structural components, drift sensitive non-structural components, and acceleration sensitive non-structural components are identified, and component-level damage assessment is performed using fragility functions determined from literature (FEMA, 2012; Dong and Frangopol, 2016). Monte Carlo simulations are conducted, and monetary losses and downtime are evaluated using consequence functions.

In the Step 3, repair actions are determined for the considered structural and non-structural components following the repair descriptions provided in fragility specifications of FEMA methodology (FEMA, 2012). Monte Carlo simulations are performed to probabilistically determine equivalent carbon emissions related to the relevant materials. The relationship between equivalent carbon emissions and the materials is extracted from (Chau et al., 2012; Dong and Frangopol, 2016). Seismic sustainability is thus evaluated by quantifying equivalent carbon emissions using the probability of damage and collapse scenarios utilizing Eqs. (1) and (2).

In Step 4, probabilistic seismic resilience can be quantified utilizing residual functionality of a building and its recovery to pre-event functionality state at the end of recovery time. The residual functionality is mapped against the different building limit states developed in Step-1; with baseline functionality at no damage and zero functionality at building collapse. Intermediate functionalities are assigned to different damage states to account for uncertainties. Recovery functions can be linear, trigonometric, exponential and depend on the community's resourcefulness and rapidity. Under an earthquake event, the building will suffer structural and non-structural damage, and building will change its state from full functionality to some residual functionality depending upon the robustness of a structure. Recovery functions are used to track time-variant functionality improvement and after the downtime the building will achieve full functionality. The time-variant functionality over investigated period can thus be determined, and resilience can be computed by integrating the time variant functionality using Eq. (3).

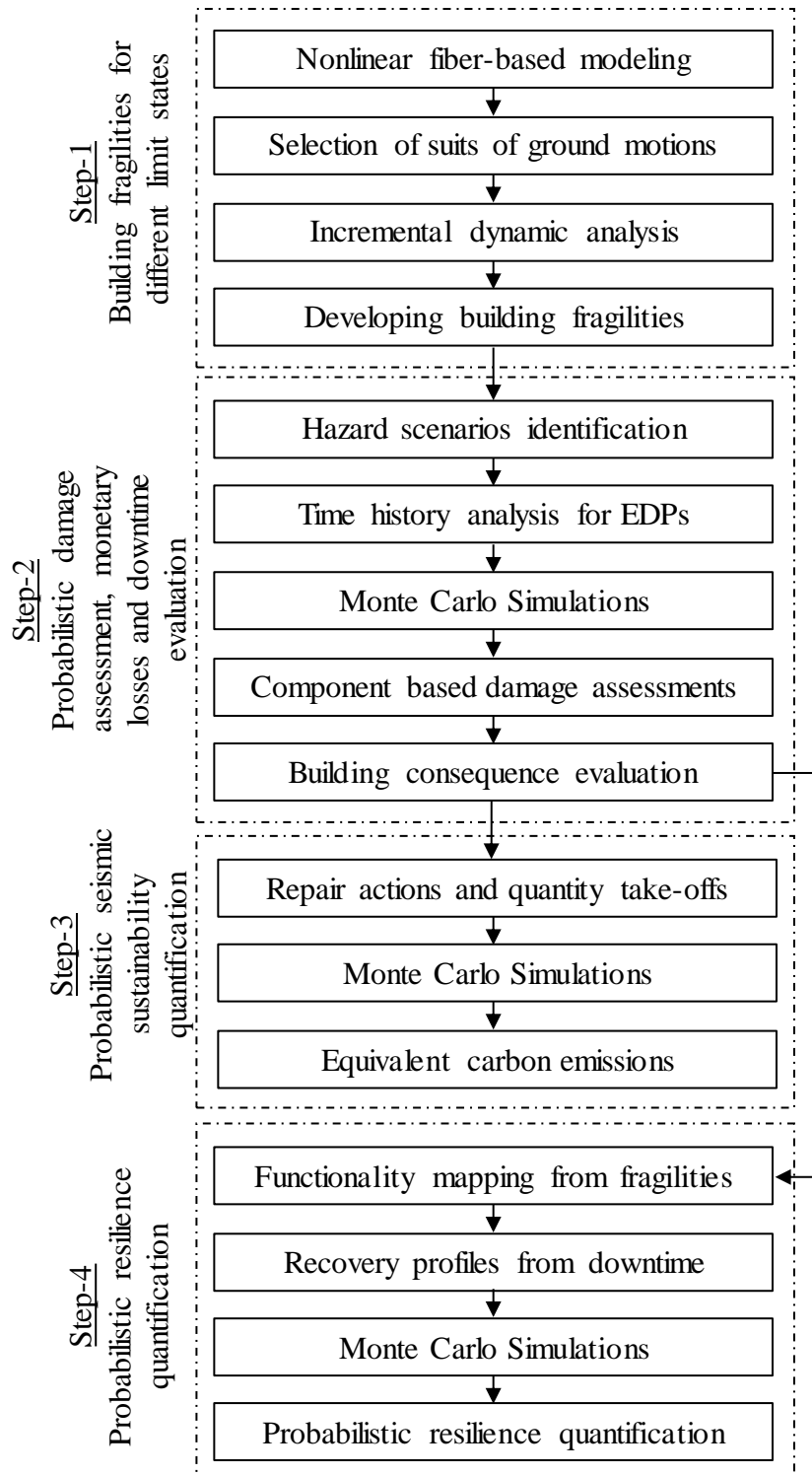


Figure 3. Probabilistic sustainability and resilience quantification framework

4. Illustrative example

4.1. Description and modeling of the investigated building

The developed integrated performance-based assessment methodology for seismic sustainability and resilience quantification is applied to an eight-story non-ductile RC moment resisting frame structure. The selected building is located in the earthquake-prone region and was not designed considering earthquake design guidelines, as a standard practice before the

implementation of earthquake codes. The non-ductile structures may perform poorly during a natural hazard since they are not designed according to the revised building codes. The building has ground floor height of 5 m and typical story height is 3.5 m, design details for critical elements along with the layout is shown in Figure 4.

The building was constructed before 1991, when UBC (1997) recommended seismic zone ‘0’ for most of the low-to-medium seismicity regions. Recent seismic hazard studies revised the seismic zones in many regions of the world, however existing building stock may be vulnerable to seismic risk. The considered building was designed only under the gravity and wind loads without considering seismic provisions. Gravity loads considered in the design process include self-weight, superimposed dead load of 4.0 kN/m² and a live load of 2.0 kN/m². The live load of 4.8 kN/m² was considered for the staircase areas and exit ways. The considered building is a residential structure and was assigned risk category II. Concrete strength of 20 MPa and mild steel with yield strength of steel of 240 MPa was used in the design. Slab thickness of 0.2m was used considering serviceability requirements and column dimensions were appropriately selected.

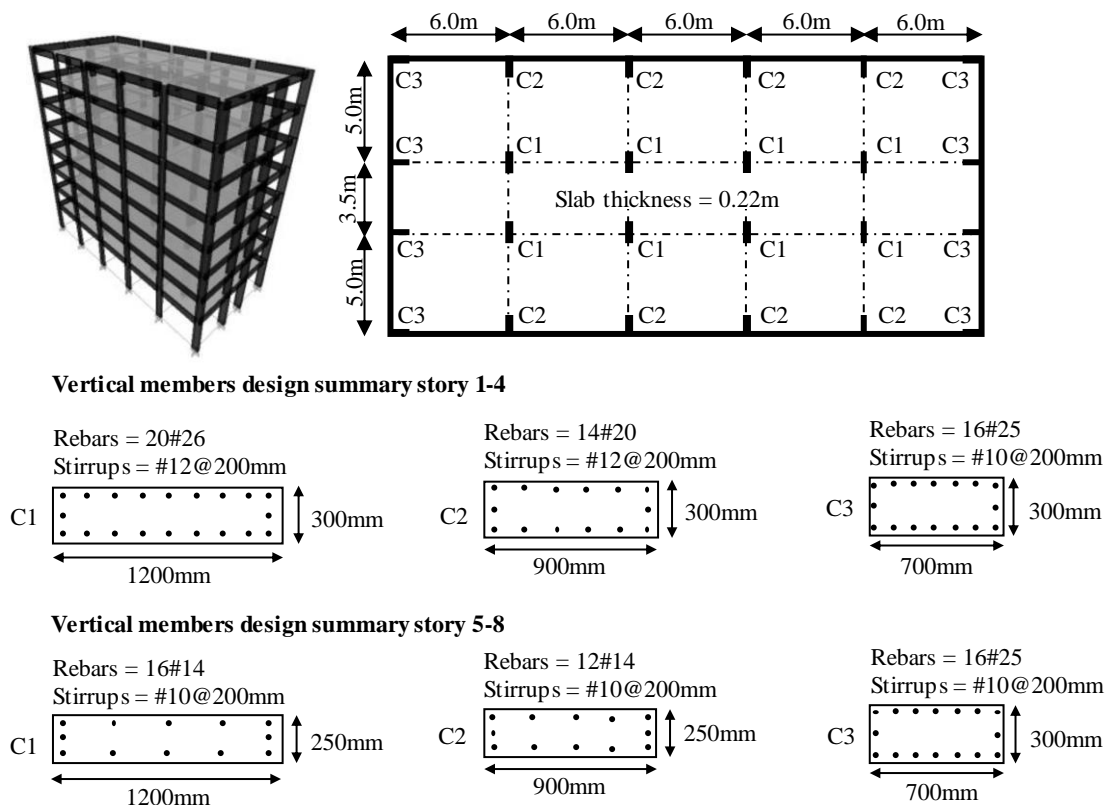


Figure 4. Vertical member design and layout of 8-story building

Fiber-based modeling technique is used for the performance evaluation of non-ductile structure under earthquake hazard. Incremental dynamic analysis was performed using nonlinear analysis software. Nonlinear material properties are used to represent concrete and steel behavior. Nonlinear concrete confinement model is used with crushing strain of 0.02 and a confinement factor of 1.05 depending upon the reinforcement detailing. A bilinear elasto-plastic model with kinematic strain hardening is used for mild steel with strain hardening parameter of 0.005, yield strength of 264 MPa, and the modulus of elasticity of 200 GPa.

Structural members are modeled using Cubic Elasto-Plastic Frame (CEPF) elements, which are capable of modeling concrete cracking and steel yielding. CEPF elements are also capable of effectively modeling nonlinear geometric and material properties in space frames (Mwafy and Elkholy, 2017).

4.2. Structural vulnerability

IDA analysis was performed using carefully selected twenty far field earthquake records based on epicentral distance, magnitude, soil conditions, PGA and a/v ratios. ASCE (2013) gives limit states with respect to Inter-story Drift Ratios (IDR) for each performance criteria. An IDR of 0.5%, 1%, and 2% is considered for IO, LS, and CP performance limit states, while numerical instability due to excessive nonlinear deformations in the structure is considered for the collapse limit state (Li et al., 2014; Vamvatsikos and Cornell, 2002). Building fragility curves developed using IDA are shown in Figure 5.

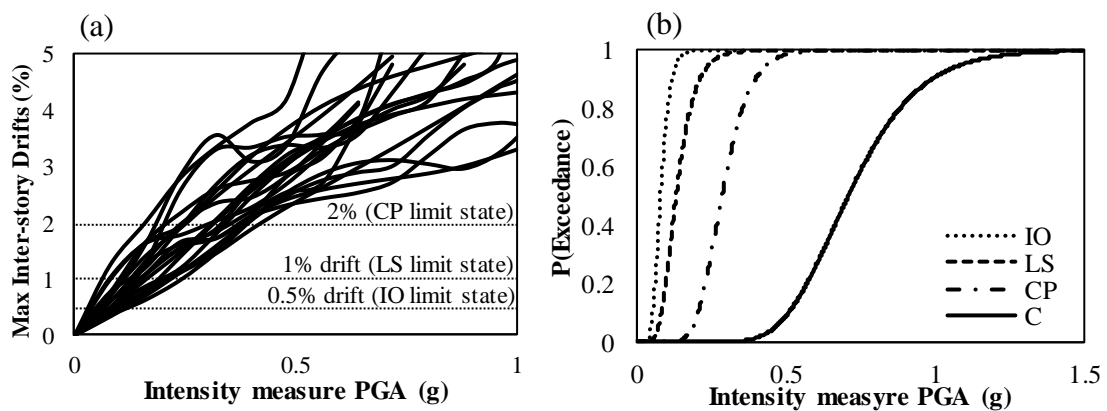


Figure 5. (a) IDA results and (b) Fragility curves of the investigated RC building

Loma Prieta-Emeryville 1989 with a magnitude of 6.93 and a duration of 28 seconds is selected for seismic sustainability and resilience assessment. The hypothetical seismic scenarios (i.e., service level earthquake (SLE) with a 50% probability of occurrence in the 50-year life of a structure, design level earthquake (DLE) with 10% probability of occurrence and maximum considered earthquake (MCE) with 2% probability of occurrence) are then assumed. The earthquake record is selected for the illustrative purposes. Generally, record to record variability and uncertainty should be considered and wide range of realizations considering uncertainties must be generated to account of ground motion variations. Time history analysis is performed, and results are plotted for maximum IDRs, and accelerations as shown in Figure 6. Maximum IDR of 1.02%, 2.47%, and 3.67% is observed at story-5 and story-6 for three earthquake scenarios. Similarly, maximum floor accelerations of 0.276g, 0.448g, and 0.570g are observed at story-8, story-3, and story-1, respectively.

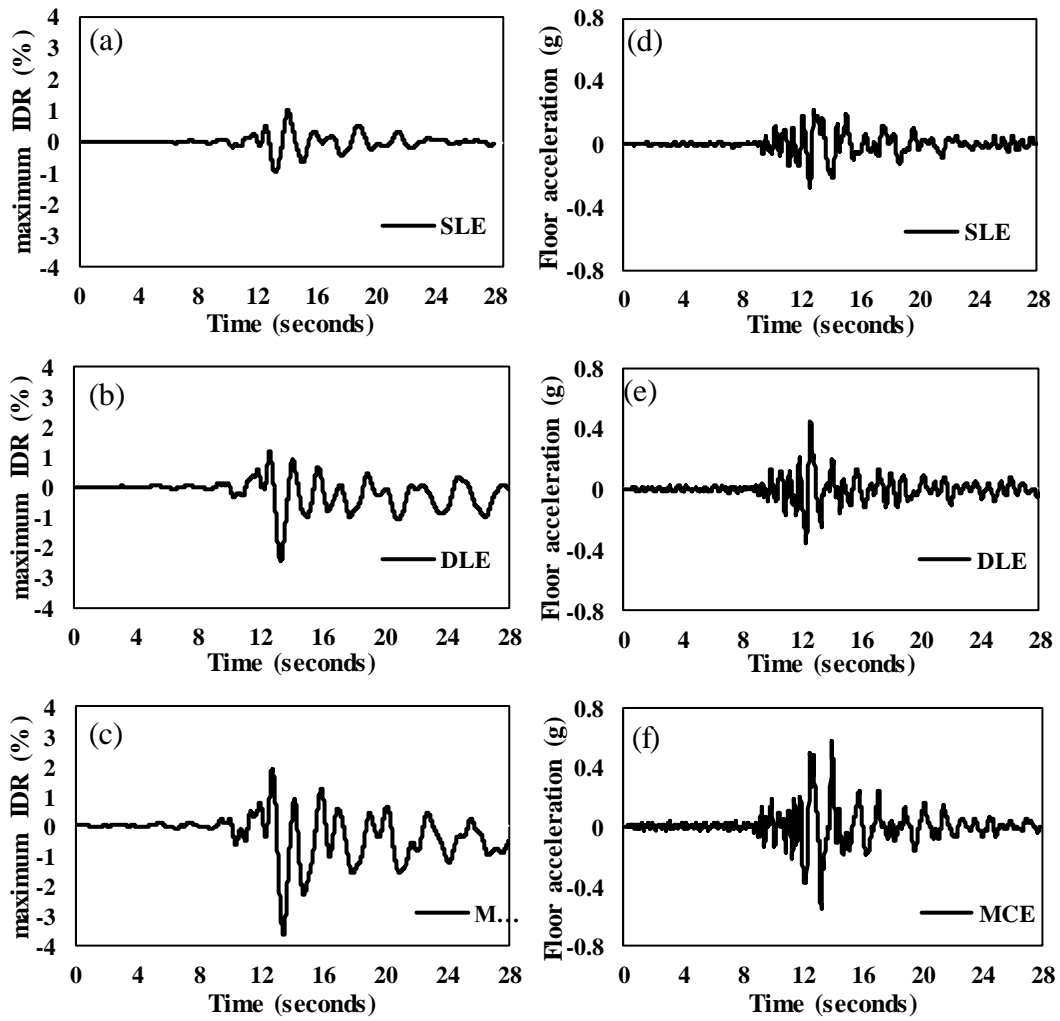


Figure 6. Time histories of inter-story drifts at (a) story-5 under SLE scenario, (b) story-5 under DLE scenario, and (c) story-6 under MCE scenario and time histories of maximum accelerations at (d) story-8 under SLE scenario, (e) story-3 under DLE scenario, and (f) story-1 under MCE scenario

As shown in Figure 7, it can be observed that increasing intensity of earthquake scenarios results in increasing demands on a structure. Peak IDRs increase by 58.48% for DLE and 32.63% for MCE. Similarly, for peak floor accelerations, an increase of 38.36% for DLE and 23.33% for MCE is observed.

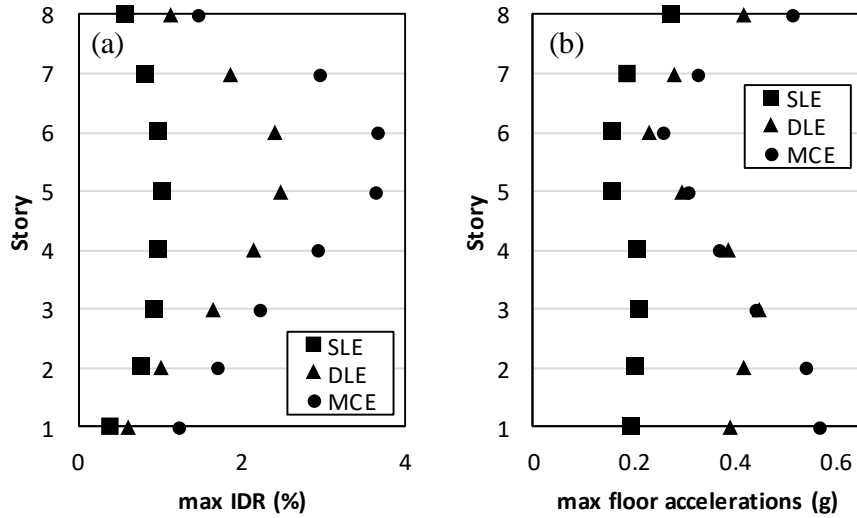


Figure 7. EDPs for earthquake scenarios (a) Peak inter-story drift ratios and (b) peak floor acceleration

4.3. Performance, seismic loss, and sustainability

Seismic loss and sustainability in terms of dollar, downtime, and equivalent carbon emissions are assessed considering structural and non-structural components. Damageable components are identified and divided into two performance groups (i.e., drifts-based performance group and acceleration-based performance group). Drifts-based performance group include drift sensitive structural components and drift sensitive non-structural components, while acceleration-based performance group includes acceleration sensitive non-structural components. The fragility functions of the damageable components are represented using lognormal distributions with median and dispersion values. Table 1 shows various structural and non-structural damageable components considered in this example with uncertainty incorporated repair costs at different damage states. The damageable components fragility curves and repair costs are collected from Cardone and Perrone (2017) and FEMA (2012).

Table 1. Fragility curves and repair costs of the damageable components

Components	Damage state	No. per floor	EDP	Fragility functions		Repair cost (USD)	
				median	dispersion	median	dispersion
Structural components							
External joints	DS1	16	IDR (%)	1.75	0.40	2090	0.39
	DS2			2.25	0.40	3180	0.32
	DS3			3.22	0.40	3860	0.30
OMRF columns	DS1	24	IDR (%)	1.50	0.40	2090	0.39
	DS2			1.75	0.40	3180	0.32
	DS3			2.00	0.40	3860	0.30
Non-structural infill components							
Masonry infill	DS1	10	IDR (%)	0.15	0.5	570	0.22
	DS2			0.40	0.5	1200	0.44
	DS3			1.75	0.35	5760	0.52
Exterior masonry infill with windows	DS1	16	IDR (%)	0.1	0.5	570	0.30
	DS2			0.3	0.5	1020	0.46

	DS3			1.75	0.4	4320	0.52
Interior masonry infill with doors and windows	DS1	12	IDR (%)	0.2	0.50	510	0.28
	DS2			0.5	0.40	960	0.46
	DS3			1.75	0.35	4650	0.52
Aluminum-framed window	DS1	30	IDR (%)	1.6	0.29	69.6	0.2
	DS2			3.2	0.29	348	0.2
	DS3			3.6	0.27	696	0.2
Non-structural MEP components							
Conveying cold water	DS1	67.5*	PFA (g)	1.5	0.4	50	0.76
	DS2	10001 f		2.6	0.4	500	0.4
Conveying hot water	DS1	954*	PFA (g)	0.55	0.4	50	0.76
	DS2	10001 f		1.1	0.4	500	0.41
Sanitary waster piping	DS1	545*	PFA (g)	1.2	0.5	80	0.58
	DS2	10001 f		2.4	0.5	560	0.34
Electrical service and distribution (Switchgear)	DS1	3.6* AP 225	PFA (g)	1.28	0.4	1940	0.16
Electrical service and distribution (Distribution panel)	DS1	3.6* AP 225	PFA (g)	2.16	0.45	1940	0.16

*DS1 = Damage state 1, DS2 = Damage state 2 and DS3 = Damage state 3

*PFA = Peak floor accelerations

*MEP= Mechanical, electrical and plumbing

*OMFR = ordinary moment resisting frame

*lf = linear foot

Fragility functions and repair functions for different damage states are presented for considered damageable components. The number of components per floor is also given. It can be noted that Mechanical, electrical and plumbing (MEP) components are acceleration sensitive, while non-structural infills and structural components are drift sensitive. The repair loss of the components is calculated using Eq. (2). The loss distributions for all the components are determined using Monte Carlo simulations and aggregated for structural and non-structural repair losses. Figure 8 shows structural and non-structural repair losses under considered seismic scenarios.

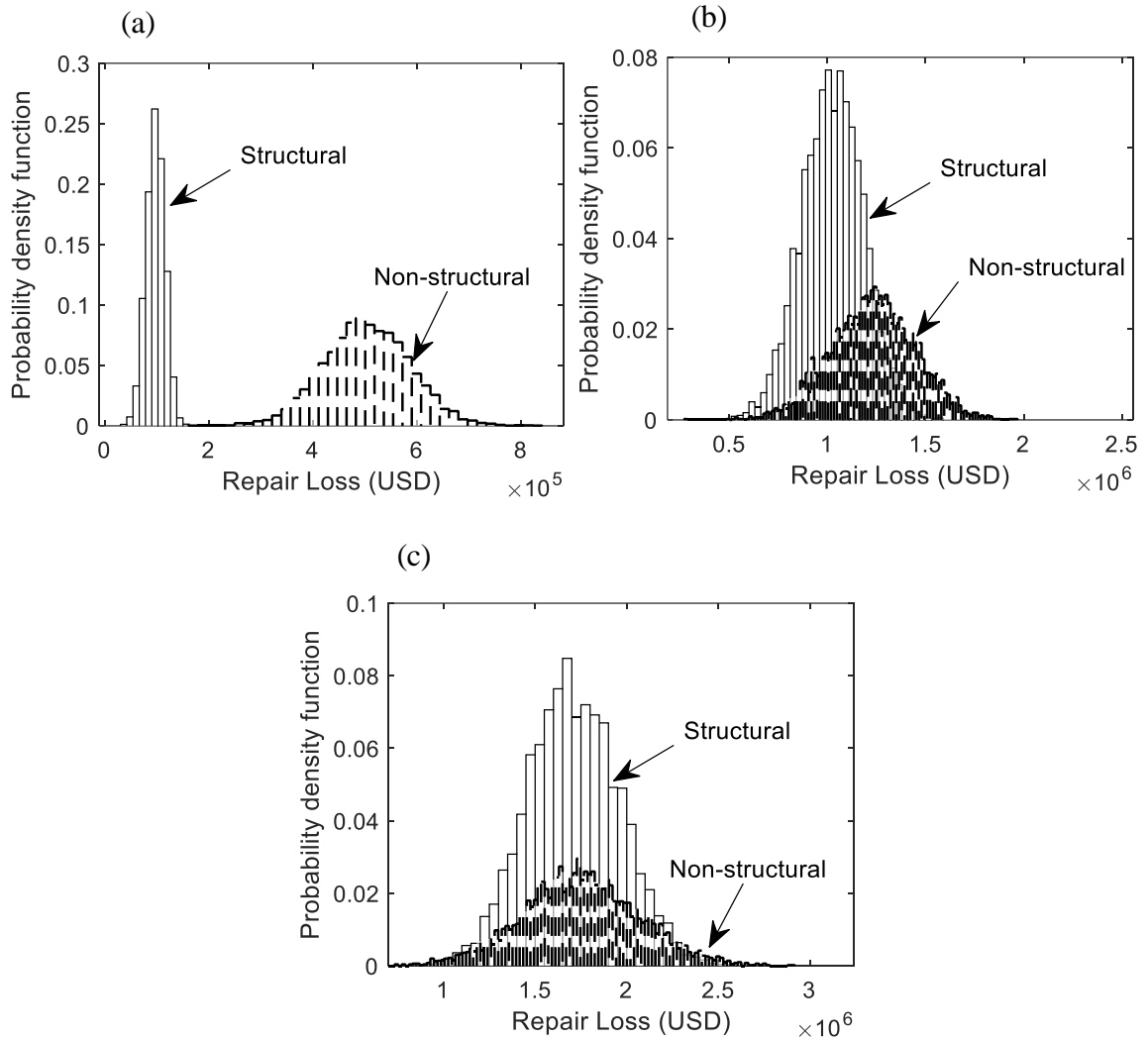
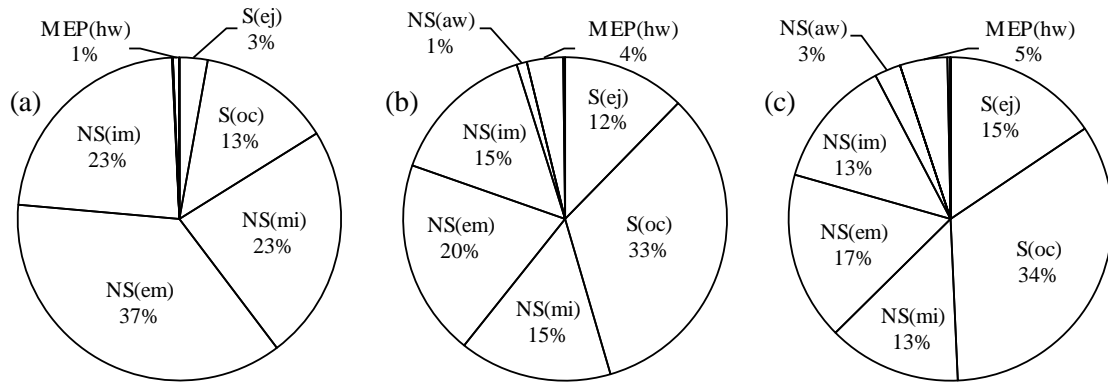


Figure 8. Distributions for repair loss associated with structural and non-structural components at (a) SLE, (b) DLE, and (c) MCE

The total expected losses for SLE, DLE, and MCE level earthquakes are 6.03×10^5 , 2.25×10^6 , and 3.47×10^6 USD, respectively. As indicated, the repair losses for the non-structural components are much larger at SLE level, but as the intensity of earthquake ground motion increases, the structural losses significantly increase along with the non-structural components. Since its non-ductile structure with stringent drift performance limit states, structural losses are also higher. The collapse cost determined at three earthquake levels is 1.72×10^0 , 5.01×10^4 , and 9.93×10^5 USD, respectively. Results indicate negligible collapse losses at SLE, 2.18% and 22.25% of the total losses at DLE and MCE. It shows that most of the structural and non-structural losses are at low probability of collapse, even at MCE level earthquake for a building designed without considering earthquake forces, the losses due to collapse contribute to 22.25%. The repair to replacement cost ratio for three earthquake levels is 15.51%, 57.84%, and 89.19%. The higher repair to replacement ratio can be due to non-ductile code configurations of the evaluated RC frame structure. The disaggregated losses are shown in the Figure 9 for three earthquake levels. It is observed that most of the damage is from non-structural infills, structural components also contribute to the repair loss considerably, while repair loss due to MEP components is negligible.



S(ej) = External joints, S(oc) = OMRF Columns, NS(mi) = Masonry infill, NS(em) = Exterior Masonry Infill with windows, NS(im) = Interior Masonry Infill with doors and windows, NS(aw) Aluminum-framed window, MEP(cw) = Conveying cold water, MEP(hw) = Conveying hot water, MEP(sw) = Sanitary waster piping, MEP(ed) = Electrical service and distribution (Switchgear), MEP(ep) = Electrical service and distribution (Distribution panel)

Figure 9. Risk disaggregation at level (a) SLE, (b) DLE, and (c) MCE

Structural repair losses are also calculated from building fragility curves and compared with the component-level damage assessment. Damage ratios required for various damage states for system level repair loss estimation are taken from Foltz (2004) as shown in Table 2. The repair losses calculated using damage ratios, building replacement cost and PoEs of building fragility curves are 1.19×10^5 , 9.35×10^5 , and 1.44×10^6 USD for three scenarios, respectively. The maximum percentage difference of 18.91% is observed for the component-level and system-level damage assessment methods using given damage ratios. The results suggest that the loss associated with component-level assessment is relatively larger than that of system level assessment approach.

Table 2. Damage ratios corresponding to different damage states

Damage State	Damage ratio (%)	Central damage Ratio
Slight Structural Damage (IO)	1.25-7.50	3.5
Moderate Structural Damage (LS)	7.5-20	10
Severe Structural Damage (CP)	20-90	65
Collapse (C)	90-100	95

Environmental impact in terms of greenhouse gases (GHG) is assessed by quantifying equivalent CO₂ emissions associated with the repair activities. Repair actions of damageable components for different damage states shown in Table 3 are used to quantify materials during repair activities. The material types of damageable building components, material take off and the relevant distributions of equivalent carbon emissions are shown in Table 4.

Table 3. Repair actions of damageable components at different damage states

Components	Damage states	Repair actions
Structural components		
	DS1	Patch new plaster and paint

External joints and OMRF Columns	DS2	Restore concrete 1 inch beyond the exposed reinforcing steel, Patch new plaster and paint
	DS3	Replace component
Non-structural infill components		
Masonry Infill	DS1	Patch new plaster and paint
	DS2	Restore broken bricks, patch new plaster and paint
	DS3	Reinstall windows and doors, restore all bricks, patch new plaster and paint
Non-structural MEP components		
Conveying cold water, hot water and sanitary piping	DS1	Fix minor leakage
	DS2	Fix one pipe break per 1000 feet
Electrical service and distribution (Switchgear and distribution panel)	DS1	Fix inoperability

The material take offs are based on the building drawings and repair actions; and the carbon emission values are based on the study conducted by Chau et al. (2012) and Dong and Frangopol (2016). Monte Carlo simulations are performance and equivalent CO₂ emissions are quantified for all the damageable components and aggregated to get total emissions. The equivalent CO₂ emissions for SLE, DLE, and MCE are shown in Figure 10.

Table 4. Material take offs and CO₂ emissions of different building materials

Material type	SLE kg	DLE kg	MCE kg	Type of PDF	CO ₂ emissions (kg CO ₂ /kg)	
					Median	β
Concrete	1.27 x10 ⁴	1.84 x10 ⁵	3.22 x10 ⁵	uniform	0.045	0.06
Steel	9.96 x10 ²	1.68 x10 ⁴	3.04 x10 ⁴	lognormal	0.460	0.4
Plaster	1.08 x10 ⁵	1.81 x10 ⁵	2.22 x10 ⁵	lognormal	0.023	0.4
Paint	8.84 x10 ³	1.33 x10 ⁴	1.57 x10 ⁴	lognormal	1.665	0.4
Brick	3.54 x10 ⁵	9.60 x10 ⁵	1.31 x10 ⁶	lognormal	0.042	0.4
Glass	4.15 x10 ²	4.05 x10 ³	6.27 x10 ³	normal	0.184	0.4
Plywood	3.17 x10 ²	4.84 x10 ³	7.50 x10 ³	lognormal	0.192	0.4

* β = dispersion values

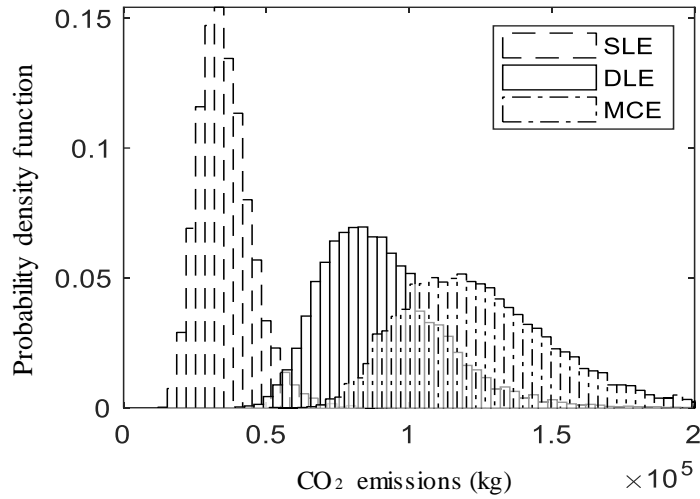


Figure 10. CO₂ emissions under three earthquake scenarios

The median values of CO₂ emissions for three earthquake scenarios are 3.447×10^4 , 8.696×10^4 , and 1.222×10^5 kg, respectively. The increase in carbon emissions from SLE to DLE is 60.36% and from DLE to MCE is 28.84%. The disaggregated carbon emissions for considered damageable components are shown in Figure 11.

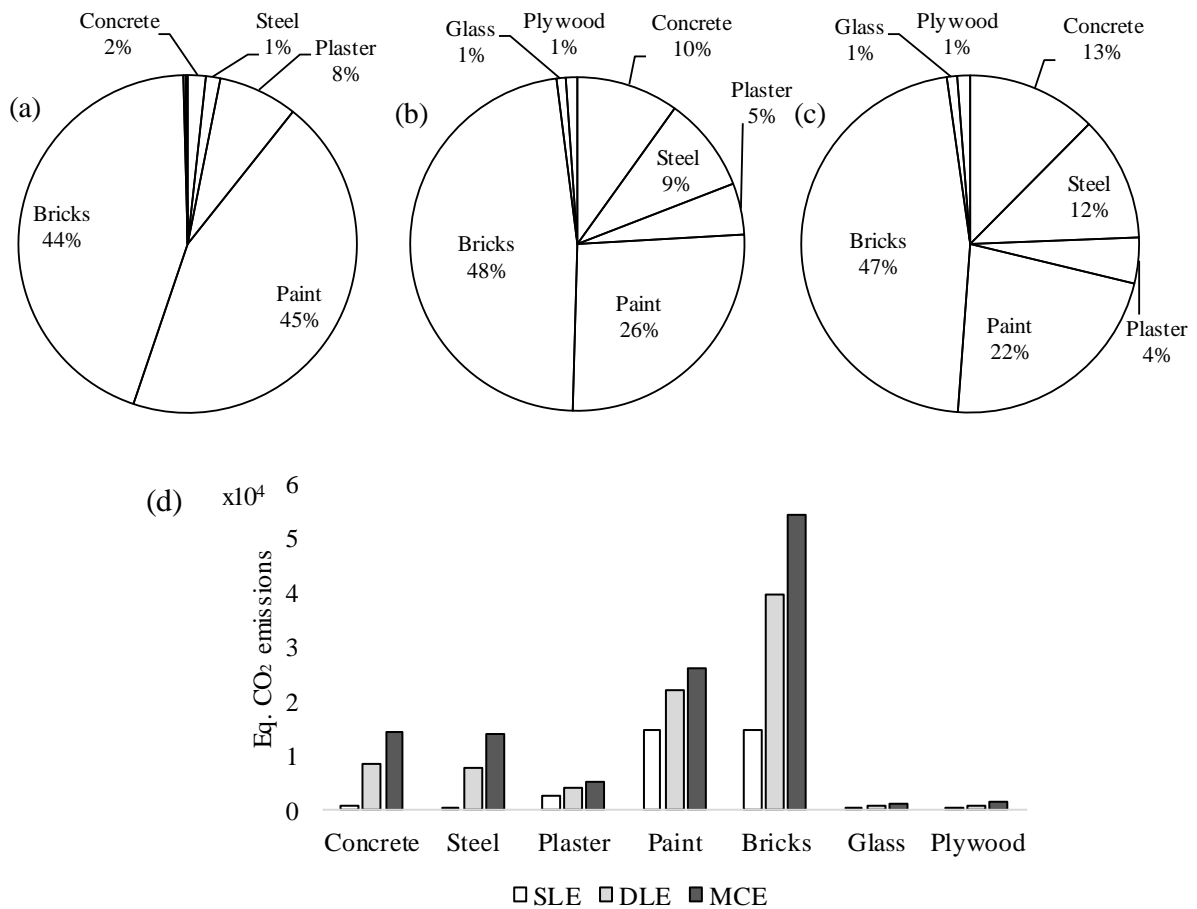


Figure 11. Disaggregated carbon emissions at (a) SLE, (b) DLE, (c) MCE, and (d) Three scenarios

Bricks and paint material used during the repair actions have high contributions to carbon emissions mostly, since bricks have low median values of damage and paint material have high carbon emissions per kg of the material used. At SLE, bricks and paint material comprise almost 89% of the carbon emissions, while at DLE and MCE concrete, steel and plaster materials also contribute to carbon emissions, but still bricks and paint have major contributions. In this example, based on the repair to replacement cost ratio at DLE and MCE, the building might be demolished and rebuilt, but if environmental impact is considered, it is comparatively environment friendly to repair a structure even at MCE level. Hence, there is a bias for whether to rebuild or repair a structure considering environmental impact. It is therefore important to incorporate sustainability impacts for a better-informed decision from social, environmental, and economic standpoint of view.

4.4. Downtime and resilience

Repair times associated with damageable components are shown in the Table 5. Repair times are represented as worker days required to complete repairs, while building downtime is the total time required for a building to complete all repairs. Downtime is calculated using two schemes (i.e., parallel (fast-track) and series (slow-track)). In practice, neither parallel or series configuration is utilized but it covers a wide range of downtime, and actual downtime is presumed to be within this range. In addition to repair times for actual building repair activities, additional time called delay time is also considered in the downtime assessment. Delay time is an additional time required for inspection, engineering mobilization, review and/or redesign, financing, contractor mobilization and permitting etc. The delay times can vary considerably and can range from weeks to months (Hutt et al., 2015). The repair times of damageable components are collected from FEMA (2012).

Table 5. Probabilistic repair times of damageable components

Components	Damage state	Repair time (Worker-days)	
		median	dispersion
Structural components			
External joints	DS1	18.9	0.46
	DS2	28.7	0.40
	DS3	35.3	0.39
OMRF columns	DS1	18.9	0.46
	DS2	28.7	0.40
	DS3	35.3	0.39
Non-structural infill components			
Masonry infill	DS1	18.9	0.46
	DS2	28.7	0.40
	DS3	35.3	0.39
Exterior masonry infill with windows	DS1	5	0.4
	DS2	10	0.4
	DS3	15	0.4
Interior masonry infill with doors and windows	DS1	5	0.4
	DS2	12	0.4

	DS3	17	0.4
Aluminum-framed window	DS1	0.18	0.3
	DS2	0.72	0.3
	DS3	1.44	0.3
Non-structural MEP components			
Conveying cold water	DS1	0.307	0.80
	DS2	0.281	0.48
Conveying hot water	DS1	0.370	0.80
	DS2	0.281	0.48
Sanitary waster piping	DS1	0.424	0.63
	DS2	3.02	0.42
Electrical service and distribution (Switchgear)	DS1	2.18	0.3
Electrical service and distribution (Distribution panel)	DS1	2.18	0.3

Slow track and fast track repair schemes can provide reasonable estimate of lower and upper bounds of a building downtime and can be calculated by dividing the total repair time with the total number of workers available per floor for repairs and adding delay times. The consequence functions for structural and non-structural components are based on (Cardone and Perrone, 2017; Dong and Frangopol, 2016; FEMA, 2012).

Figure 12 shows the downtime at three earthquake levels for slow track and fast track. The expected downtime for the slow track at three levels is 567, 1735, and 2621 days, respectively; similarly, for fast track is 90, 362, and 486 days. The difference between slow and fast track depends on the number of stories along with other factors, as the number of stories increases, the difference in the slow-track and fast-track increases considerably (Almufti and Willford, 2013).

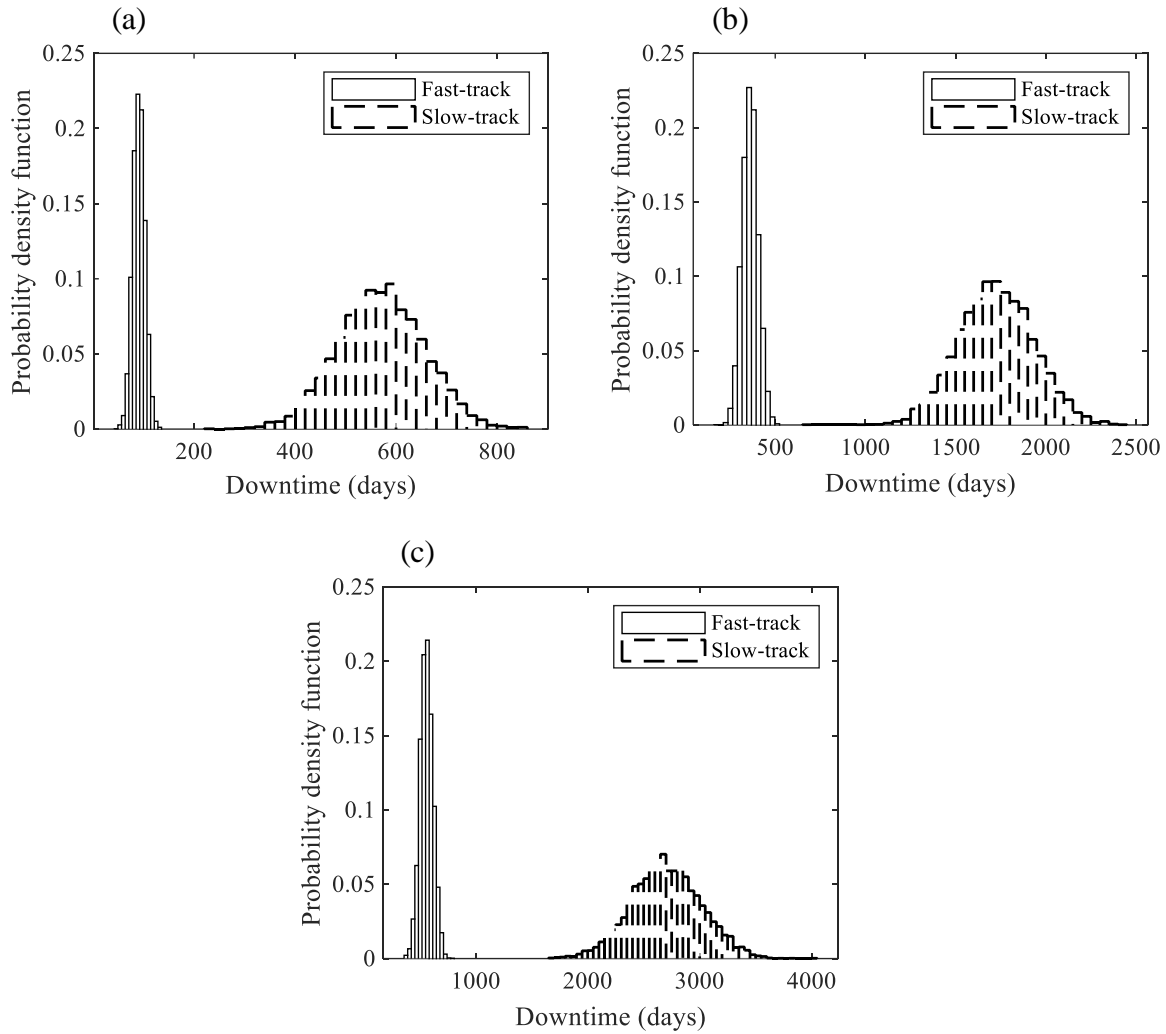
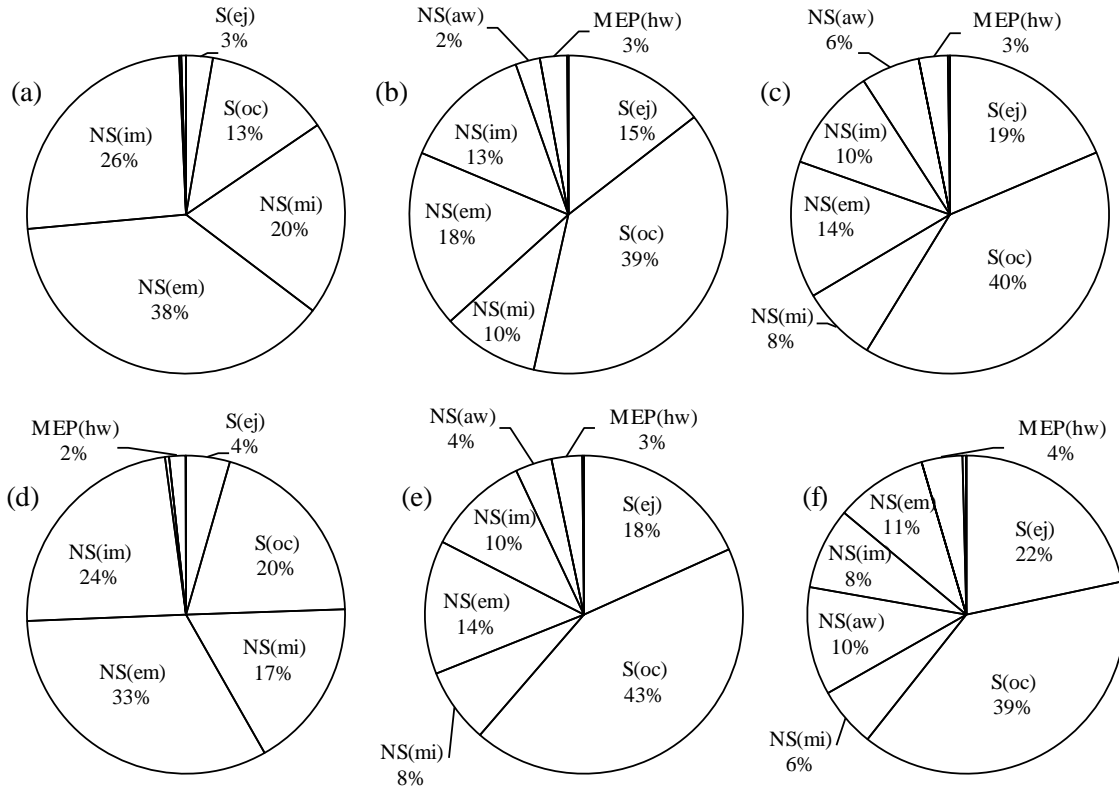


Figure 12. Downtime for slow and fast track at levels (a) SLE, (b) DLE, and (c) MCE

The disaggregated downtimes for structural, non-structural, and MEP components are shown in the Figure 13 for three earthquake levels.



S(ej) = External joints, S(oc) = OMRF Columns, NS(mi) = Masonry infill, NS(em) = Exterior Masonry Infill with windows, NS(im) = Interior Masonry Infill with doors and windows, NS(aw) Aluminum-framed window, MEP(cw) = Conveying cold water, MEP(hw) = Conveying hot water, MEP(sw) = Sanitary waster piping, MEP(ed) = Electrical service and distribution (Switchgear), MEP(ep) = Electrical service and distribution (Distribution panel)

Figure 13. Downtime disaggregation for slow-track at level (a) SLE, (b) DLE, (c) MCE and for fast-track at level (d) SLE, (e) DLE, (f) MCE

In the SLE level, most of the downtime is due to the non-structural repair of infills, while for DLE and MCE levels, downtime due to structural repair is dominant. The distribution of downtime is utilized for the resilience assessment. Performance limit states (i.e., IO, LS, CP, and collapse) are considered for the determination of residual functionality. Residual functionality also considered as the robustness of a building system can be quantified from the building performance limit states. The uncertainties associated with functionality are incorporated using triangular distribution with lower bound, upper bound and mode corresponding to IO, LS, and CP as (0.7, 0.9, 0.8), (0.4, 0.6, 0.5), and (0, 0.2, 0), respectively (Dong and Frangopol, 2016). The residual functionality corresponding to no damage is 1 and for collapse of a building is 0. Monte Carlo simulations are performed for the uncertainty modeling of residual functionality against different limit states and corresponding expected values for three levels are determined (i.e., 0.52, 0.22, and 0.15 for SLE, DLE, and MCE). Residual functionalities are used to calculate resilience under investigated time interval using Eq. (1). The calculated resilience at investigated time interval of 100, 200, and 300 days is shown in Figure 14 for fast-track and slow-track.

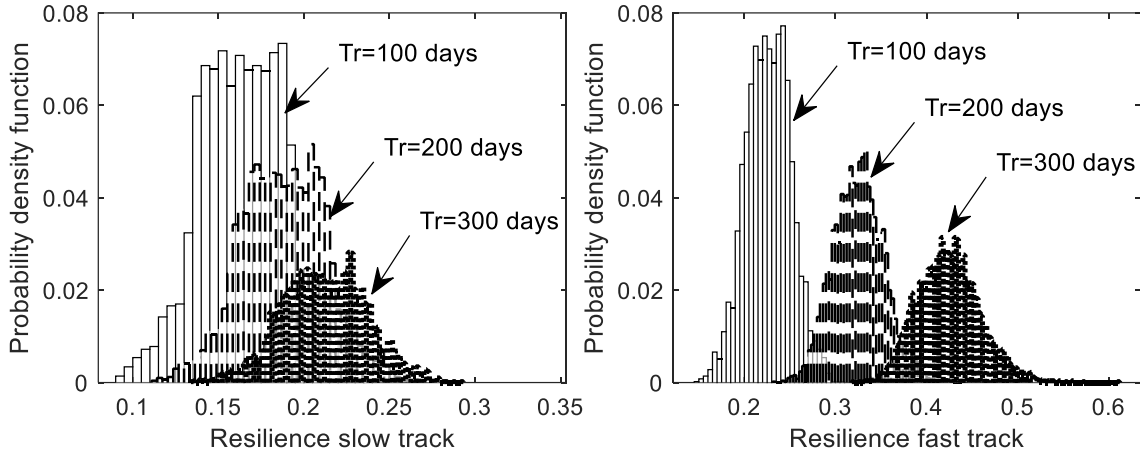


Figure 14. Distributions of resilience at investigated 100, 200 and 300 days under DLE

The expected values of resilience are plotted in Figure 15 for the investigated time period of 1,000 days.

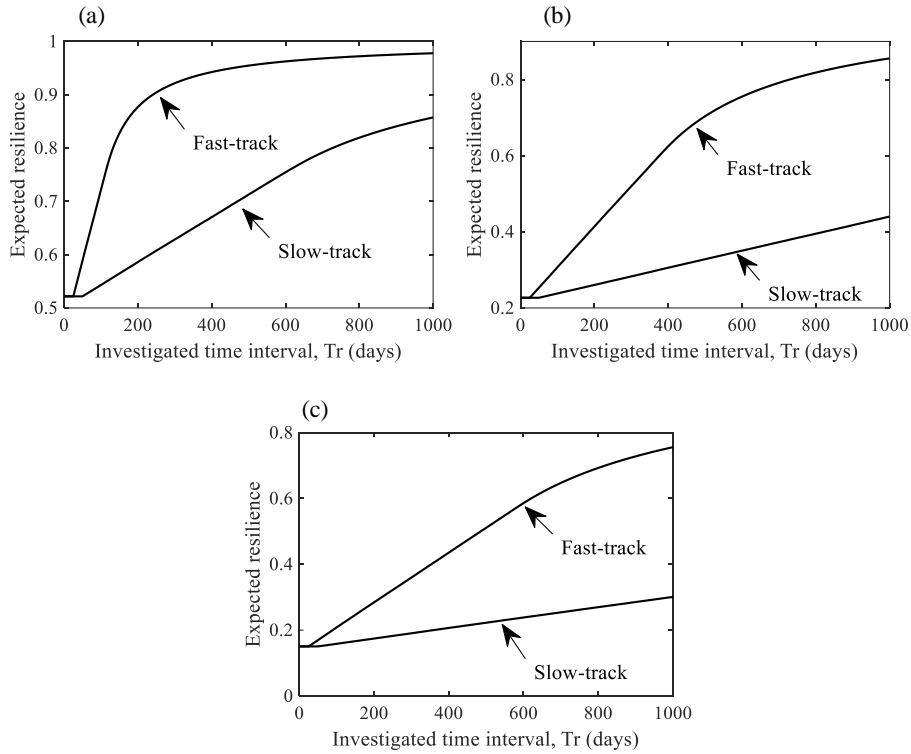


Figure 15. Expected resilience under 1000 days investigated period under (a) SLE, (b) DLE, and (c) MCE

As indicated, the residual functionalities are substantially low for DLE and MCE. The reduced residual functionality shows poor earthquake performance during an earthquake event. The comparatively large differences between slow-track and fast-track downtimes increase the bounds, but still useful information can be deduced about the recovery profile of a building. The expected resilience of 0.975, 0.85, and 0.75 is observed for fast-track at investigated time period of 1000 days, while for slow-track the expected resilience observed is 0.86, 0.42, and 0.31, respectively.

5. Conclusions

The paper provides a probabilistic framework to compute seismic sustainability and resilience using performance-based assessment methodology. The uncertainties associated with structural performance and consequence functions are incorporated. Distributed repair loss, equivalent carbon emissions, and downtime are calculated. The residual functionalities are determined probabilistically, and resilience is quantified for investigated time period. The proposed approach is illustrated on a non-ductile RC frame structure.

Following conclusions are drawn.

1. Performance-based methodology is used for the repair and downtime assessment of non-ductile RC building. Monetary losses due to non-collapse account for 99.99%, 97.82%, and 77.75% of the total losses at three earthquake scenarios. The total repair losses for structural and non-structural components at three levels are 9.72×10^4 , 1.02×10^6 , 1.71×10^6 USD and 5.06×10^5 , 1.23×10^6 , 1.76×10^6 USD. Non-structural infills contribution to repair loss is found to be significant with 83%, 51%, and 46% of the total repair loss. Losses due to structural components also dominate with 45% and 49% at DLE and MCE.
2. The equivalent carbon emissions for three earthquake levels equal 3.447×10^4 , 8.696×10^4 , and 1.222×10^5 kg, respectively. The emissions are dominated by bricks and paint material with 89%, 74%, and 69% of the total emissions at three earthquake scenarios. Repair to replacement ratio for economic loss at three scenarios is 15.51%, 57.84% and 89.19% while, for environmental is 10.59%, 26.80%, and 37.39%. In the considered example, it is environment friendly to repair a structure even at MCE earthquake scenario.
3. Resilience quantification using performance-based assessment methodology can be used as an indicator for measuring robustness and recovery of a building infrastructure. Based on results, the non-ductile building suffers high loss of functionality and is not able to gain even 50% of the functionality at DLE and MCE for slow-track after 1000 days of investigated time period, showing poor performance not only during an earthquake but during the recovery time as well. Fast-track scheme shows considerably better recovery performance but for that community must have high resourcefulness and rapidity attributes.
4. Downtime assessment plays an important role in the resilience assessment of individual multi-story buildings and thus should be investigated further to improve quantification of resilience, since neither series or parallel repair schemes would be adopted for the repair of an actual building after an earthquake. The results conclude huge variability in slow-track and fast-track resilience and should follow a logical repair strategy for downtime assessment to reduce variability.
5. Future research is needed to incorporate record-to-record variability using large suits of earthquake records for assessment purposes. Improved uncertainty modeling and functionality mapping should be developed for better predicting residual functionality during and after an earthquake.

References

- Alipour A and Shafei B (2016) Seismic resilience of transportation networks with deteriorating components. *Journal of Structural Engineering* 142(8): C4015015.
- Almufti I and Willford M (2013) REDi™ Rating System: Resilience Based Earthquake Design Initiative for the Next Generation of Buildings. Version 1.0. October, Arup.
- Ambraseys N, Smit P, Douglas J, et al. (2004) European strong-motion data. *Bollettino di geofisica teorica ed applicata* 45(3): 113-129.
- ASCE (2013) Seismic evaluation and retrofit of existing buildings.
- Asprone D and Manfredi G (2015) Linking disaster resilience and urban sustainability: a global approach for future cities. *Disasters* 39(s1): s96-s111.
- Bocchini P, Frangopol DM, Ummenhofer T, et al. (2013) Resilience and sustainability of civil infrastructure: Toward a unified approach. *Journal of Infrastructure Systems* 20(2).
- Broccardo M, Galanis P, Esposito S, et al. (2015) Probabilistic resilience assessment of civil systems: Analysis and validity of the PEER framework. *Safety and Reliability of Complex Engineered Systems: ESREL* 331.
- Brundtland GH (1987) *Report of the World Commission on environment and development: "our common future."*. United Nations.
- Bruneau M, Chang SE, Eguchi RT, et al. (2003) A framework to quantitatively assess and enhance the seismic resilience of communities. *Earthquake Spectra* 19(4): 733-752.
- Burton HV, Deierlein G, Lallemand D, et al. (2015) Framework for incorporating probabilistic building performance in the assessment of community seismic resilience. *Journal of Structural Engineering* 142(8): C4015007.
- Cardone D and Perrone G (2017) Damage and loss assessment of pre-70 RC frame buildings with FEMA P-58. *Journal of Earthquake Engineering* 21(1): 23-61.
- Carvalho R, Buzna L, Bono F, et al. (2014) Resilience of natural gas networks during conflicts, crises and disruptions. *PloS one* 9(3): e90265.
- Chau C, Hui W, Ng W, et al. (2012) Assessment of CO2 emissions reduction in high-rise concrete office buildings using different material use options. *Resources, conservation and recycling* 61: 22-34.
- Dong Y and Frangopol DM (2016) Performance - based seismic assessment of conventional and base - isolated steel buildings including environmental impact and resilience. *Earthquake Engineering Structural Dynamics* 45(5): 739-756.
- Dong Y and Frangopol DM (2017) Probabilistic assessment of an interdependent healthcare-bridge network system under seismic hazard. *Structure and Infrastructure Engineering* 13(1): 160-170.
- Dong Y, Frangopol DM and Saydam D (2013) Time - variant sustainability assessment of seismically vulnerable bridges subjected to multiple hazards. *Earthquake Engineering & Structural Dynamics* 42(10): 1451-1467.
- duPont IV W and Noy I (2015) What happened to Kobe? A reassessment of the impact of the 1995 earthquake in Japan. *Economic Development and Cultural Change* 63(4): 777-812.
- Ellingwood BR (2006) Mitigating risk from abnormal loads and progressive collapse. *Journal of Performance of Constructed Facilities* 20(4): 315-323.
- FEMA (2012) Seismic Performance Assessment of Buildings: Vol. 1—Methodology. Reportno. Report Number|, Date. Place Published|: Institution|.
- Foltz R (2004) Estimating seismic damage and repair costs. *Advisor: Dr. Mary Beth Hueste.*
- Frangopol DM, Dong Y and Sabatino S (2017) Bridge life-cycle performance and cost: analysis, prediction, optimisation and decision-making. *Structure and Infrastructure Engineering* 13(10): 1239-1257.

- Gencturk B, Hossain K and Lahourpour S (2016) Life cycle sustainability assessment of RC buildings in seismic regions. *Engineering Structures* 110: 347-362.
- Hashemi MJ, Al-Attraqchi AY, Kalfat R, et al. (2019) Linking seismic resilience into sustainability assessment of limited-ductility RC buildings. *Engineering Structures* 188: 121-136.
- Herrera M, Abraham E and Stoianov I (2016) A graph-theoretic framework for assessing the resilience of sectorised water distribution networks. *Water Resources Management* 30(5): 1685-1699.
- Hutt CM, Almufti I, Willford M, et al. (2015) Seismic loss and downtime assessment of existing tall steel-framed buildings and strategies for increased resilience. *Journal of Structural Engineering* 142(8): C4015005.
- Katsanos EI, Sextos AG and Manolis GD (2010) Selection of earthquake ground motion records: A state-of-the-art review from a structural engineering perspective. *Soil Dynamics and Earthquake Engineering & Structural Dynamics* 30(4): 157-169.
- Kishida T, Contreras V, Bozorgnia Y, et al. (2018) NGA-Sub ground motion database.
- Koliou M, van de Lindt JW, McAllister TP, et al. (2017) State of the research in community resilience: progress and challenges. *Sustainable and Resilient Infrastructure*. 1-21.
- Li Y, Song R and Van De Lindt JW (2014) Collapse fragility of steel structures subjected to earthquake mainshock-aftershock sequences. *Journal of Structural Engineering* 140(12): 04014095.
- Lin P and Wang N (2017a) Stochastic post-disaster functionality recovery of community building portfolios I: Modeling. *Structural Safety* 69: 96-105.
- Lin P and Wang N (2017b) Stochastic post-disaster functionality recovery of community building portfolios II: Application. *Structural Safety* 69: 106-117.
- Marchese D, Reynolds E, Bates ME, et al. (2018) Resilience and sustainability: Similarities and differences in environmental management applications. *Science of the Total Environment* 613.
- Masoomi H and van de Lindt JW (2018) Community-Resilience-Based Design of the Built Environment. *ASCE-ASME Journal of Risk and Uncertainty in Engineering Systems, Part A: Civil Engineering* 5(1): 04018044.
- Miles SB and Chang SE (2006) Modeling community recovery from earthquakes. *Earthquake Spectra* 22(2): 439-458.
- Mwafy A and Elkholy S (2017) Performance assessment and prioritization of mitigation approaches for pre-seismic code structures. *Advances in Structural Engineering* 20(6): 917-939.
- Padgett JE and Li Y (2014) Risk-based assessment of sustainability and hazard resistance of structural design. *Journal of Performance of Constructed Facilities* 30(2): 04014208.
- Padgett JE and Tapia C (2013) Sustainability of natural hazard risk mitigation: Life cycle analysis of environmental indicators for bridge infrastructure. *Journal of Infrastructure Systems* 19(4): 395-408.
- Qeshta IM, Hashemi MJ, Gravina R, et al. (2019) Review of resilience assessment of coastal bridges to extreme wave-induced loads. *Engineering Structures* 185: 332-352.
- Rodriguez-Nikl T (2015) Linking disaster resilience and sustainability. *Civil Engineering and Environmental Systems* 32(1-2): 157-169.
- Sabatino S, Frangopol DM and Dong Y (2015) Sustainability-informed maintenance optimization of highway bridges considering multi-attribute utility and risk attitude. *Engineering Structures* 102: 310-321.
- Sfahani M, Guan H and Loo Y-C (2015) Seismic reliability and risk assessment of structures based on fragility analysis—a review. *Advances in Structural Engineering* 18(10): 1653-1669.

- Sun W, Bocchini P and Davison BD (2018) Resilience metrics and measurement methods for transportation infrastructure: the state of the art. *Sustainable and Resilient Infrastructure*. 1-32.
- UBC (1997) Uniform building code. *International Conference of Building Officials, Whittier, CA*.
- Vamvatsikos D and Cornell CA (2002) Incremental dynamic analysis. *Earthquake Engineering and Structural Dynamics* 31(3): 491-514.
- Wen W, Zhang M, Zhai C, et al. (2019) Resilience loss factor for evaluation and design considering the effects of aftershocks. *Soil Dynamics and Earthquake Engineering* 116: 43-49.
- Zhai C-H, Wen W-P, Li S, et al. (2015) The ductility-based strength reduction factor for the mainshock–aftershock sequence-type ground motions. *Bulletin of Earthquake Engineering* 13(10): 2893-2914.
- Zhao X, Li W and Stanbrook J (2014) A framework for the integration of performance based design and life cycle assessment to design sustainable structures. *Advances in Structural Engineering* 17(4): 461-470.
- Zheng Y and Dong Y (2018) Performance-based assessment of bridges with steel-SMA reinforced piers in a life-cycle context by numerical approach. *Bulletin of Earthquake Engineering*. 1-22.
- Zheng Y, Dong Y and Li Y (2018) Resilience and life-cycle performance of smart bridges with shape memory alloy (SMA)-cable-based bearings. *Construction and building materials* 158: 389-400.